From Electric Field Dependent Particle Dynamics to Bistability in the Breakdown of the Quantum Hall Effect *

J. Riess

Centre de Recherches sur les Très Basses Températures,
Centre National de la Recherche Scientifique, B.P. 166, F-38042 Grenoble Cedex 9

Z. Naturforsch. **50a**, 1090–1096 (1995); received August 16, 1995

The integer quantum Hall effect (IQHE) and its breakdown (onset of dissipation) reflect general properties of the solutions of the time-dependent Schrödinger equation, where the macroscopic electric field $\boldsymbol{E}$ is properly included. In particular, the dynamics of an electron in a broadened Landau band not only depends on the disorder potential but also on the value of $|\boldsymbol{E}|$. This leads to an $|\boldsymbol{E}|$-dependence of the conductivities σ_{xx} and σ_{xy}, which implies that the IQHE breaks down if $|\boldsymbol{E}|$ is sufficiently high. We show that the general form of the $|\boldsymbol{E}|$-dependence of σ_{xx} and σ_{xy} can lead to jumps in the longitudinal resistance at the breakdown of the IQHE, as observed in recent experiments.

Key words: Quantum Hall effect, breakdown, bistability, electrical field dependent conductivities.

Introduction

In the integer quantum Hall effect (IQHE) [1] one observes wide plateaux of the Hall conductivity σ_{xy} as a function of the filling factor of the impurity broadened Landau levels (or equivalently, as a function of the applied perpendicular magnetic field B). In the plateau region σ_{xy} has the quantized value $\sigma_{xy} = ne^2/h$, n integer. Simultaneously the dissipative conductivity σ_{xx} vanishes. This is true, provided the temperature is sufficiently low and the sample current is not too high. If the current increases, the width of the conductance plateaux shrinks, until they disappear entirely at values of the current corresponding to an electric field strength of the order of 100 $\mathrm{V\,cm^{-1}}$ [2]. These experimental facts are consistent with theoretical results [3, 4] which show that the IQHE itself, and in particular its breakdown, are a direct consequence of the *electric field dependence* of the dynamic properties of the states in a broadened Landau band. More recent experiments [5, 6] seem to confirm that the macroscopic electric field in the sample is the crucial parameter in the breakdown phenomena.

Very recently, the breakdown of the IQHE has been investigated more closely by several experimental groups. In particular, sudden jumps in the dissipative resistance have been observed for filling factors ν close to integer values, e.g. $\nu = 2$ [7–10]. The resistance jumps were quantized and showed a time-dependent behaviour.

This interesting breakdown behaviour has been investigated in detail on an AlGaAs heterojunction in the Hall bar configuration with a *constricted* current path of width 50 μm, where the following effects have been observed [9]: For filling factors ν slightly smaller than two the dissipation resistance $R_x = U_x(I)/I$ changes from "zero" to a much higher value within a small range of the current I. This change at certain values of I and the magnetic field B is sharp, i.e., the resistance R_x immediately jumps from its low ("zero") value to its high value. The system is able to leave the dissipative state to switch back to $R_x \approx 0$. If I and B are kept fixed the system switches between these two states. On increasing the sample current slightly, the average time during which the system is in the dissipative state increases until at a certain value of I only the dissipative state remains, i.e., no further switching is observed. For a given filling factor ν the height of the resistance jumps is constant (quantized). In [9] switching between a non-dissipative and a dissipative state has been observed only for filling factors $1.97 > \nu > 1.9$. In this range of ν the height of the resistance jumps was roughly proportional to $2-\nu$. A similar filling factor dependence has been observed in [7].

In order to understand the observed phenomena, a previously developed electron heating model [11] for the onset of dissipation has been suggested. However, as will be discussed below, this model does not seem

* Paper presented at the 5th Annual Meeting of ENGADYN, Grenoble, October 10–13, 1994.

Reprint requests to Dr. J. Riess.

0932-0784 / 95 / 1200-1090 $ 06.00 © – Verlag der Zeitschrift für Naturforschung, D-72027 Tübingen

to explain the asymmetry with respect to $\nu=2$ of the observed switching behaviour, nor the filling factor dependence of the resistance jumps, nor the fact, that the jumps always start at "zero" resistance (when the current increases).

In this paper we propose a different explanation of the resistance jumps at the breakdown of the IQHE, and in particular those observed in [7] and [9]. Our explanation is a consequence of the general microscopic theory of the IQHE developed by the author over the last four years [3, 4, 12]. There it has been shown that the conductance behaviour of each electron in the broadened Landau band not only depends on the disorder potential but also on the strength $|\boldsymbol{E}|$ of the macroscopic electric field $\boldsymbol{E}$ at the position of the electron. The breakdown phenomena are macroscopic manifestations of the $|\boldsymbol{E}|$-dependence of the microscopic electron dynamics, and may be considered as a further confirmation of the theoretical results obtained in [3, 4, 12]. In Sect. 2 we shortly review the basic elements of this theory and collect the results which are relevant for our purpose. In Sect. 3 these are applied to explain the microscopic origin of the resistance jumps. Section 4 contains a discussion of the filling factor dependence of the jumps. Finally, in the appendix we investigate the consistency between our theory and the experimental values of the resistance jumps obtained in [9].

2. Electric Field Dependent Particle Dynamics and Conductivities in a Broadened Landau Band

The starting point of a microscopic theory of the IQHE is the Hamiltonian

$$H = [1/(2m)]\{(\hbar/i)\nabla - (e/c)\boldsymbol{A}(\boldsymbol{r})\}^2 + V(\boldsymbol{r}) - e\boldsymbol{E}\boldsymbol{r}. \tag{1}$$

Here $V(\boldsymbol{r})$, $\boldsymbol{r}=(x,y)$, is a static substrate potential which contains homogeneous disorders. $\boldsymbol{B}=(0,0,B)=\operatorname{curl}\boldsymbol{A}(\boldsymbol{r})$ is the magnetic field perpendicular to the x-y-plane. $\boldsymbol{E}$ is a homogeneous electric field, i.e., H describes a subdomain of a macroscopic sample, over which the electric field $\boldsymbol{E}(\boldsymbol{r})$ can be considered constant.

In the presence of a realistic disorder potential $V(\boldsymbol{r})$ the Schrödinger equation

$$[H - i\hbar\partial_t]\psi = 0 \tag{2}$$

cannot be solved exactly. Most theories of the IQHE have assumed a linear response approximation. However, the electric field dependence of the conductivities immediately outside the conductance plateaux, i.e., in the breakdown regime, indicate that such an assumption is not justified.

In the following we will not make such an assumption. We will point out some general properties of the exact solutions of (2), where the macroscopic electric field $|\boldsymbol{E}|$ is properly included.

First we remark that in the presence of a homogeneous electric field $\boldsymbol{E}$ and of a disorder potential $V(x,y)$ (which varies in *both* spatial directions) no stationary solutions of (2) exist [13] (although (1) does not contain the time explicitly). This important result indicates that the process of electric conductance in the IQHE is intrinsically time-dependent.

This result can be understood in another way by performing the time-dependent gauge transformation

$$\boldsymbol{A}'(\boldsymbol{r},t) = \boldsymbol{A}(\boldsymbol{r}) + \nabla f(\boldsymbol{r},t), \quad \psi' = \psi\exp[ief/(\hbar c)], \quad f'(\boldsymbol{r},t) = -c\boldsymbol{E}\boldsymbol{r}t, \tag{3}$$

whence

$$(H' - i\hbar\partial_t)\psi' = 0. \tag{4}$$

The Hamiltonian

$$H' = [1/(2m)]\{(\hbar/i)\nabla - (e/c)\boldsymbol{A}'(\boldsymbol{r},t)\}^2 + V(\boldsymbol{r}) \tag{5}$$

depends explicitly on time (note that H' coincides with H if $\boldsymbol{E}=0$).

The energies ε_s in the broadened Landau bands are determined by the stationary solutions of (1) or (4) in the absence of $\boldsymbol{E}$: $H[\boldsymbol{E}=0,\ V(x,y)]\psi_s=\varepsilon_s\psi_s$. We consider that this problem has been solved and we ask how the states ψ_s change when $\boldsymbol{E}$ is different from zero, and what are the corresponding velocity components parallel and perpendicular to $\boldsymbol{E}$. The former determine the dissipative conductivity σ_{xx} and the latter the Hall conductivity σ_{xy}.

It has been found [13] that for each state ψ_s two limits exist: 1. For sufficiently low $|\boldsymbol{E}|$ the macroscopic velocity parallel to $\boldsymbol{E}$ vanishes. 2. For sufficiently high $|\boldsymbol{E}|$ the Hall velocity of the state tends towards the value $v_d=c|\boldsymbol{E}|/B$ (i.e. to the classical value in the absence of the disorder potential $V(x,y)$).

The low $|\boldsymbol{E}|$-limit corresponds to the adiabatic [14] limit of the time-dependent Schrödinger equation (4). The adiabatic solutions are momentary eigenfunctions of $H'[V(x,y),\boldsymbol{E},t]$. Due to the absence of symmetry (presence of disorder) the corresponding ener-

gies $\varepsilon_s(t)$ do not intersect [15]. In addition, in a macroscopic system the levels $\varepsilon_s(t)$ are closely spaced. It follows then from the general relation

$$\begin{aligned} \partial_t \langle \psi' | H' \psi' \rangle &= e \boldsymbol{E} \langle \psi' | \boldsymbol{v}'_{\mathrm{op}} | \psi' \rangle \\ &= e \boldsymbol{E} \langle \psi | \boldsymbol{v}_{\mathrm{op}} | \psi \rangle \end{aligned} \tag{6}$$

that the velocity component parallel to $\boldsymbol{E}$ of an adiabatic state rapidly oscillates around zero and therefore does not contribute to the macroscopic current.

The existence of the high $\boldsymbol{E}$-limit can be proved [13, 4] by transforming (2) to a frame of reference which moves with the drift velocity $\boldsymbol{v}_d = (c/B^2)\boldsymbol{E} \times \boldsymbol{B}$. In the transformed equation the electric field $\boldsymbol{E}$ vanishes and the disorder potential moves with the constant velocity $-\boldsymbol{v}_d$. The high $|\boldsymbol{E}|$-limit is reached when the solution of the transformed Schrödinger equation is in the so-called sudden approximation limit [14]. This limit occurs whenever $v_d = c|\boldsymbol{E}|/B$ is sufficiently high (the solution feels then only some time average of the moving disorder potential). The Hall velocity of the back transformed sudden approximation solution is just $\boldsymbol{v}_d$.

In the adiabatic regime the velocity $\langle \boldsymbol{v}_{\mathrm{op}} \rangle$ of a state is highly non-linear with respect to $\boldsymbol{E}$ and t. If a state is in the intermediate regime (between the adiabatic and the high-$\boldsymbol{E}$-limit), its velocity is the sum of a linear and a nonlinear (non-classical) term. (This follows from general considerations and has been confirmed by detailed calculations using model disorder potentials, where the time-dependent wave functions could be obtained in a very good approximation [16]). When $|\boldsymbol{E}|$ increases further, the nonlinear term decreases until it completely disappears in the high-$\boldsymbol{E}$-limit. The width of the conductance plateaux in the quantum Hall regime is a measure for the total non-linear fraction of the velocities of the conducting states in a broadened Landau band. This non-linear fraction shrinks to zero in the high-$\boldsymbol{E}$-limit. When all the states in the band are in their high-$\boldsymbol{E}$-limit, the width of the conductance plateaux is zero. (This shows that the quantum Hall regime is partly nonlinear on the microscopic level!)

When the Fermi level is in a range of adiabatic levels, the total energy (in the representation H') of the system does not increase with time. Hence, according to (6) no net current parallel to $\boldsymbol{E}$ is possible, i.e., the dissipative conductivity vanishes. On the other hand, when $\boldsymbol{E}$ is increased such that the states near ε_F are no longer in the adiabatic limit, i.e., when nonadiabatic transitions between the levels near ε_F occur, the energy (in the representation H') of the system increases with time. This is equivalent to a current parallel to $\boldsymbol{E}$, hence to a nonvanishing dissipative conductivity σ_{xx}. (Dissipation occurs because the accumulated excess energy above ε_F is periodically lost to the surrounding heat bath by inelastic scattering events.)

In order to calculate the left hand side of (6) for each state, one needs to know the ($|\boldsymbol{E}|$-dependent) nonadiabatic transition probabilities between the disorder perturbed Landau levels ε_s. However, at present these transition probabilities can only be calculated in special cases, but not in the presence of an arbitrary disorder potential. Nevertheless, a qualitative measure of the transition probabilities can be obtained from an estimation of the electric "threshold" fields $E^{\mathrm{th}}(s)$ which characterize the crossover from the low $\boldsymbol{E}$-limit to the high $\boldsymbol{E}$-limit of a particular state ψ_s. $E^{\mathrm{th}}(s)$ is defined by the following inequality: a state ψ_s is in the low (high) field limit if $|\boldsymbol{E}| \ll (\gg) E^{\mathrm{th}}(s)$.

It is important to know how the values $E^{\mathrm{th}}(s)$ are distributed among the states ψ_s in a broadened Landau band (cf. Fig. 3 of [12]). It has been found [4] that states at the band edges gave the highest fields $E^{\mathrm{th}}(s)$, for which an estimation have values of the order of 100 $\mathrm{V\,cm^{-1}}$ (for typical disorder potentials). This is consistent with experimental values of the breakdown fields of the integer quantum Hall effect (IQHE). Further, the values of $E^{\mathrm{th}}(s)$ rapidly decrease from the edges towards the center of the bands, where they have been estimated to be many orders of magnitude smaller [4]. This leads to an electric field dependent mobility edge, corresponding to a decreasing width of the conductance plateaux when the total current is increased, as observed in experiments.

At a mobility edge the nonadiabatic transition probabilities start to become non-negligible. The mobility edges separate the adiabatic levels in the tails from the nonadiabatic levels in the centre of a broadened Landau band. From the foregoing it is clear that the mobility edges move towards the band tails when $|\boldsymbol{E}|$ increases. The breakdown field E_b is that value of $|\boldsymbol{E}|$ for which the Fermi level ε_F coincides with a mobility edge. Therefore E_b is highest for integer filling factors and decreases when ε_F moves towards the center of a band.

When $|\boldsymbol{E}|$ increases above E_b, σ_{xx} increases from zero to higher values until its saturation value σ^s. Here all states have reached their high-$\boldsymbol{E}$-limit.

3. Bistability in the Current Induced Breakdown of the IQHE

The constriction considered in the experiment of [9] has the dimensions $L_x = L_y = 50$ μm. For the following we denote by E_x, E_y the average electric field components in x and y direction in the constriction. Since the constriction is quite narrow with respect to the rest of the sample, we can further assume that in the constriction the current is in the x-direction. Experimentally one imposes the total current I through the sample (which in the constriction is in x-direction, $I = I_x = j_x L_y$, where j_x is the current density) and measures the potential drop which establishes itself in the system across ($U_y = E_y L_y$) and along ($U_x = E_x L_x$) the constriction. The longitudinal resistance is then obtained as $R_x = U_x/I = E_x/j_x$.

From general macroscopic considerations [17] bistabilities in a current-voltage relation are the result of a negative differential current-voltage behaviour. In the case of the experiment of [9] this means that an N-shaped j_x-E_x relation must exist. If the magnetic field B was absent, such a behaviour would necessarily imply a negative differential conductivity σ_{xx} as a function of E_x.

However, in the presence of a magnetic field *two* conductivities exist, σ_{xx} and σ_{xy}, which give two different contributions to j_x. In this case a negative differential diagonal resistivity, σ_{xx} is not indispensible to obtain an N-shaped j_x-E_x relation. In the following we show that the general behaviour of σ_{xx} and σ_{xy} (resulting from the microscopic theory, see Sect. 2 can lead to such an j_x-E_x behaviour, provided the filling factor ν is slightly *below* an integer value n.

From the general relation

$$j_x = \sigma_{xx} E_x + \sigma_{xy} E_y , \tag{7}$$

and from the fact that in the constriction we have

$$j_y = \sigma_{xx} E_y - \sigma_{xy} E_x = 0 \tag{8}$$

one obtains

$$j_x = [\sigma_{xx} + (\sigma_{xy})^2/\sigma_{xx}] E_x = (1/R_x) E_x . \tag{9}$$

Since $R_x = \varrho_{xx} L_x/L_y$, and since $L_x = L_y$ in the experimental setup, R_x is just equal to ϱ_{xx}. From (9) we see that R_x depends on both conductivities, σ_{xx} and σ_{xy}, which have different dependences on E_x. In the limit $E_x = 0$, (9) tends to $(n e^2/h) E_b$, where E_b is the breakdown field, i.e., the value of $|\boldsymbol{E}|$ where σ_{xx} starts to become different from zero. The variables R_x and E_x in (9) are directly accessible by the experiment. On the other hand, the microscopic theory discussed in Sect. 2 gives the qualitative behaviour of σ_{xx} and σ_{xy} as a function of the variable $|\boldsymbol{E}|$. Therefore we also need the following equations (which follow from (7) and (8)):

$$E_x = |\boldsymbol{E}| \sigma_{xx}/[(\sigma_{xx})^2 + (\sigma_{xy})^2]^{1/2} , \tag{10}$$

$$j_x = |\boldsymbol{E}| [(\sigma_{xx})^2 + (\sigma_{xy})^2]^{1/2} . \tag{11}$$

In the quantum Hall regime ($j_x \leq j_b$, i.e., $|\boldsymbol{E}| \leq E_b$), E_x vanishes, hence $j_x = (n e^2/h) E_y$. If $|j_x|$ increases beyond the breakdown value $j^b = (n e^2/h) E_b$, $|\boldsymbol{E}|$ increases above E_b. At $|\boldsymbol{E}| = E_b$, σ_{xx} starts to increase monotonically from zero to higher values (until saturation), hence $|E_x|$ increases as well [see (10)]. Figure 1 shows the behaviour of σ_{xx} as a function of $|\boldsymbol{E}|$. Its behaviour as a function of E_x is similar. (From (10) one obtains $\sigma_{xx} \approx E_x (n e^2/h)/E_b$ for sufficiently low values of E_x.)

On the other hand, $|\sigma_{xy}|$ monotonically *decreases* from $n e^2/h$ towards $(e^2/h)(n - \delta)$, where $n - \delta = \nu$, $\delta > 0$. (These are just the two limits of $|\sigma_{xy}|$ which are reached for $|\boldsymbol{E}| \leq E_b$ and $|\boldsymbol{E}| \gg E_b$. In the second limit the Hall velocity of each state has just the unperturbed classical value $c|\boldsymbol{E}|/B$, see Sect. 2. This leads to $|\sigma_{xy}| = (e^2/h)\nu$.) As a consequence,

$$|\sigma_{xy}| = (e^2/h)[n - \delta f(|\boldsymbol{E}|)] , \tag{12}$$

where $f(|\boldsymbol{E}|)$ increases monotonically from zero (at $|\boldsymbol{E}| = E_b$) to one (at some saturation value higher than E_b), see Figure 2.

We write $|\boldsymbol{E}| = E_b + z$. Expressing σ_{xy} in (11) by (12) leads to the equation

$$j_x = |E_b + z| \{[\sigma_{xx}(z)]^2 + (e^4/h^2)[n - \delta f(z)]^2\}^{1/2} . \tag{13}$$

From (13) it follows that under certain conditions $j_x(z)$ decreases below j_b when z increases from zero to higher values, before it increases again at higher z.

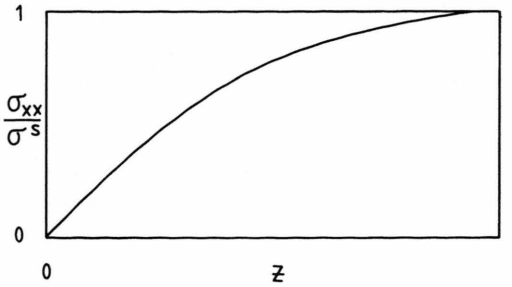

Fig. 1. Schematic behaviour of σ_{xx} as a function of $z = |\boldsymbol{E}| - E_b$. σ^s is the saturation value of σ_{xx} for $z \gg 0$.

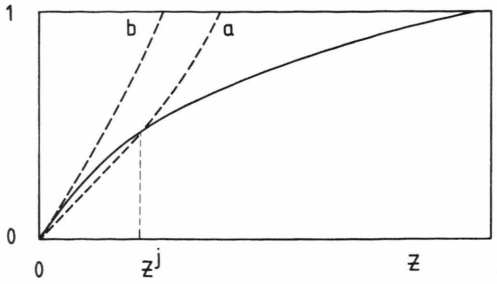

Fig. 2. Schematic illustration of the function $f(z)$ (full line). The dashed line shows the corresponding function $f^\circ(z)$, (14), for which two situations are possible: a) intersection with $f(z)$; b) no intersection.

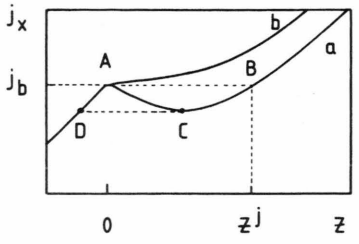

Fig. 3. Qualitative illustration of the two possible behaviours of the current j_x: a) N-shaped behaviour; b) monotonic increase with z.

To investigate this in more detail we keep $j_x = j_b$ fixed in (13) and solve the resulting equation for $f(z)$. This defines a special function $f^\circ(z)$, whose meaning is as follows: for a given $z > 0$ the value of j_x is smaller (bigger) than j_b when $f(z)$ in (12) is bigger (smaller) than $f^\circ(z)$. A simple calculation gives

$$f^\circ(z) \approx z\, n/(E_b \delta) + [\sigma_{xx}(z)\, h/e^2]^2/(2\, n\, \delta), \quad (0 < z \ll E_b). \tag{14}$$

Therefore, if $f^\circ(z)$ increases sufficiently slowly (curve (a) in Fig. 2, such that it interests with $f(z)$, the current $j_x(z)$ has an N-shaped behaviour (Figure 3a). In the opposite case (curve (b) in Fig. 2), the current j_x monotonically increases with z (Figure 3b)) i.e. no resistance jump can occur.

As we have seen above, E_x increases when z increases (for $z > 0$). Therefore j_x has an N-shaped behaviour as a function of E_x whenever it has an N-shaped behaviour as a function of z. The value z_j of Fig. 2 corresponds to point B in Figure 3. It is obtained by solving (13) for $z\,(z > 0)$, setting $j_x = j_b$ on the left hand side. The corresponding value E_x^j is then obtained by means of (10), whence

$$E_x^j = (E_b + z^j)\,\sigma_{xx}(z^j)/\{[(\sigma_{xx}(z^j)]^2 + [\sigma_{xy}(z^j)]^2\}^{1/2}. \tag{15}$$

The resistance jump is given by $R^j = E_x^j/j_b$.

Remark: Our qualitative discussion does not take account of the detailed form of $\sigma_{xx}(|\boldsymbol{E}|)$ and $f(|\boldsymbol{E}|)$ in the immediate neighbourhood of $|\boldsymbol{E}| = E_b$. The curves $\sigma_{xx}(|\boldsymbol{E}|)$ and $f(|\boldsymbol{E}|)$ actually start to increase (probably exponentially) already slightly before their steep increase in Fig. 1 and 2, i.e., the true E_b is somewhat below $z = 0$. The reason is that the mobility edge is not mathematically sharp. The present article is focussed on experiments at relatively low temperatures, where this exponential increase corresponds to a very short interval near $z = 0$. Therefore it has been neglected in our qualitative discussion (and has not been indicated in Figs. 1 and 2). Its possible consequence would be that the resistance jumps from A to B in Fig. 3 may start slightly above $R_x = 0$.

4. Discussion

At present it is not possible to make a sufficiently exact microscopic ab initio calculation of j_b and of the detailed form of $f(z)$ and of $\sigma_{xx}(z)$ such that (13) and (15) reproduce the experimental values of the R_x-jumps with sufficient accuracy. We can however draw some qualitative conclusions.

For low values of $z\,(z > 0)$ the second term on the right hand side of (14) can be neglected in a first approximation. $f^\circ(z)$ is then proportional to $1/(\delta E_b)$. Below a lower limit value of δ the function $f^\circ(z)$ is so steep that no intersection with $f(z)$ occurs and therefore no jump of R_x can occur. Such a behaviour is consistent with [9], where no resistance jumps have been observed below $\delta \approx 0.036$.

The first term on the right hand side of (14) leads to a slight decrease in the steepness of $f^\circ(z)$ when δ increases, i.e. to an increase of the intersection value z^j in Figure 2. This could explain the increase of R^j for increasing δ, which has been observed in [9] for relatively small values of δ (from $\delta \approx 0.036$ up to $\delta \approx 0.075$).

Since E_b increases with increasing δ, $1/(\delta E_b)$ decreases only for sufficiently low δ. For instance, with the experimental values E_b of [9] (see below) $1/(\delta E_b)$ decreases for increasing δ until $\delta \approx 0.07$ and then increases again. (Further, for higher δ the second term in (14) may become more important since $\sigma_{xx}(z)$ in-

creases with increasing σ^s, which is roughly proportional to δ, at least in [9], see below.) As a consequence, the increase of z^j with δ is attenuated until it is stopped, and finally this tendency is reversed. This could qualitatively explain the behaviour of R^j observed in [9] for $\delta \gtrsim 0.075$. In the appendix we will show that the values of the resistance jumps measured in [9] are compatible with this qualitative theoretical behaviour.

Our analysis shows that the existence of an intersection point z^j in Fig. 2, hence of a resistance jump R^j, depends on the detailed z-dependence of $f(z)$ and of $\sigma_{xx}(z)$. This seems to explain why such jumps have been seen only in particular samples under particular experimental conditions, even if δ was positive. Further, according to (14) the existence of an intersection point z^j seems favored by small n. This might explain why in [9] R_x-jumps are observed for $n = 2$ but not for $n = 4$.

The form of $\sigma_{xx}(z)$ and $f(z)$ implies that a jump of R_x always starts at (or near) $z = 0$, i.e., at (or near) zero resistance R_x, when the current is increased (since the system jumps from A to B in this case). This is consistent with the experimental facts of [9]. This important point seems not to follow from the heating model of [11]. In [11] and "S"-shaped σ_{xx} versus E_y relation is proposed. But the behaviour of j_x due to the decrease of $|\sigma_{xy}|$ for $E_x > 0$ or for $|\boldsymbol{E}| > E_b$ is not discussed. Further, the model of [11] seems not to explain the dependence of the R_x-jumps on the filling factor. In particular, the argument of [11] is independent of the sign of δ. This appears to be in contradiction to the observation of [9] (see also [7]), where only resistance jumps for positive δ have been observed. On the other hand, from our analysis only jumps for positive δ are possible, since for negative δ, the Hall conductivity $|\sigma_{xy}|$ monotonically increases (together with σ_{xx}), hence j_x monotonically increases as well.

When the current is *decreased* from values above j_b to a value below j_b, the system jumps from C to D in Figure 3. The corresponding resistance jump $R^{CD} = E_x^C/j_D$ is expected to be smaller than the corresponding resistance jump R^j from A to B (since $E_x = 0$ for $z \leq 0$). This should be investigated in future experiments*.

In this article we have shown that resistance jumps are caused by the fact that σ_{xx} and σ_{xy} change with different signs as a function of a parameter. Instead of E_x or $|E|$ as discussed above, this parameter can also be ν(B). In this case j_x is fixed and j_b changes due to the change of ν. When ν decreases such that j_b attains the value of j_x, (i.e., such that ε_F crosses a mobility edge), resistance jumps can occur according to our analysis, provided this mobility edge is situated at a fraction δ *below* a fully occupied band. This effect has been observed in [7]. The measured resistance jumps showed a similar dependence on δ as in [9], in agreement with our theoretical analysis.

We have not discussed the time-dependence of the switching behaviour. This would need an analysis which includes the electric circuit of the experimental setup.

In [8] and [10] more complicated voltage step structures, with a more complicated time-dependent behaviour have been observed. These experiments deal with bigger samples, where the voltage is measured over a distance of mm (while the constrictions used in [7] and [9] are 50 μm to 300 μm long). The measured voltage structures seem to be a superposition of contributions from smaller domains which may be comparable to those investigated in [7] and [9]. It is therefore possible, that the observed effects are caused by the same basic mechanism as discussed in Section 3. This is in particular suggested by the fact that in [10] the voltage steps have been observed only on the high magnetic field side of the $n = 2$ plateau, in agreement with our theory. However, a quantitative explanation of the observed effects would need a more macroscopic analysis.

Acknowledgements

The author thanks the participants of the meeting at the Col du Cucheron, in particular J. Peinke, for helpful and stimulating discussions. Further thanks go to F. J. Ahlers for critical and constructive comments and to H. Scherer for sending a preliminary version of his thesis.

Appendix

In the experiments of [9] the resistance jumps appear for $\nu = 2 - \delta$, $\delta > 0$. The value of j_b as a function of δ can be taken from Fig. 1 of [9]. This gives values

* *Note added in proof*: Recently we received an extract of the thesis of H. Scherer (PTB, Braunschweig), where experiments are reported which confirm this prediction.

which decrease from $j_b = 1.02$ A/m for $\delta = 0.036$ to $j_b = 0.496$ A/m for $\delta = 0.09$ (this decrease of j_b with increasing δ is in qualitative agreement with the general microscopic theory reviewed in Section 2). Further, by extrapolating the curves in Fig. 1 of [9] we have guessed the saturation value ϱ^s of ϱ_{xx} as a function of δ. We thus obtained the relation $\varrho^s \approx 6414\delta - 58$ [Ω]. From the relations $\sigma^s_{xx} \approx (\sigma^s_{xy})^2 \varrho_{xx}$ and $\sigma^s_{xy} = (2e^2/h)(1 - 0.5\delta)$ we get

$$\sigma^s \approx (4e^4/h^2)(1-\delta)(6414\delta - 58),\ 0.02 \lesssim \delta \lesssim 0.11\,. \quad (16)$$

(σ^s increases with δ because the density of states at the Fermi level increases with δ). From (10) we obtain for sufficiently low z

$$\sigma_{xx}(z^j) \approx E^j_x (2e^2/h)/E_b\,. \quad (17)$$

[From Fig. 1 it is reasonable to assume that the linear approximation (17) is valid for $\sigma_{xx}(z)/\sigma^s \lesssim 0.6$.] Further, $\sigma_{xx}(z)/\sigma^s$ has a behaviour close to $f(z)$ (see above), i.e., in a crude approximation we have

$$f(z) \approx \sigma_{xx}(z)/\sigma^s\,. \quad (18)$$

We expect that the intersection value $f(z^j)$ is sufficiently below the saturation value $f = 1$, say $f(z^j) \lesssim 0.6$ (cf. Figure 2). From this and from (17) and (18) we get

$$\sigma_{xx}(z^j)/\sigma^s \approx E^j_x (2e^2/h)/(\sigma^s E_b) \lesssim 0.6\,. \quad (19)$$

We have verified that the inequality (19) is fulfilled by the experimental values of [9]. We found that $\sigma_{xx}(z^j)/\sigma^s$ increases from 0.31 (for $\delta = 0.036$) to 0.34 (for $\delta = 0.07$) and then decreases again to reach 0.29 at $\delta = 0.09$. This behaviour is consistent with the general δ-dependence of z^j and of $f(z^j)$ discussed in Section 4. As an example, consider the case $\delta = 0.06$, which corresponds to the following experimental values (see above): $E^j_x = 148.8$ V/m, $j_b = 0.74$ A/m, hence $E_b = 9600$ V/m, $(2e^2/h)\sigma^s \approx 21$. If we put these values into the right hand side of (19), we obtain

$$\sigma_{xx}(z^j)/\sigma^s \approx 0.325\,, \quad (20)$$

which satisfies the inequality (19). Further, from (14) we obtain

$$f^o(z) \approx 0.0035\, z \quad (\text{for } \delta = 0.06,\ z \lesssim z^j) \quad (21)$$

(assuming that the second term in (14) can be neglected for $\delta = 0.06$, $z \lesssim z^j$). From (18), (20), (21), and $f(z^j) \approx f^o(z^j)$ we get $z^j \approx 93$ V/m.

These estimations show that the experimental results of [9] are consistent with reasonable functions $\sigma_{xx}(z)$, $f(z)$ or $\sigma_{xx}(E_x)$, $f(E_x)$. From (9) we were able to reproduce the measured resistance jumps R^j as a function of δ (Fig. 6 of [9]) using the functions $\sigma_{xx}(\xi) = \sigma^s F(\xi)$, $f(\xi) = F(\xi)$, where $\xi = E_x(2e^2/h)/(E_b\sigma^s)$ and $F(\xi) = \tanh(\xi) + [\tanh(b\xi) - \tanh(\xi)]^2$ (b varying from 1.284 for $\delta = 0.036$ to 1.09 for $\delta = 0.09$). Note that $\sigma^s F(\xi)$ has the correct initial derivative for small $E_x(\sigma_{xx} \approx E_x(2e^2/h)/j_b$, which follows from (10) for E_x tending to zero). The parameter b has the effect of slightly changing the curvature with respect to $\tanh(\xi)$. The linear part of $R^j(\delta)$ in Fig. 6 of [9] could be quite well reproduced by using a single function $F(\xi)$ (with $b = 1.236$) in (9), i.e. by just changing σ^s and δ in the expression for σ_{xy}.

[1] K. von Klitzing, G. Dorda, and M. Pepper, Phys. Rev. Lett. **45,** 494 (1980).
[2] G. Ebert, K. von Klitzing, K. Ploog, and G. Weimann, J. Phys. C **16,** 5441 (1983). For a review of experimental aspects see M. A. Cage in "The Quantum Hall Effect", R. E. Prange and S. M. Girvin, Eds., Springer-Verlag, New York 1990.
[3] J. Riess, Phys. Rev. B **41,** 5251 (1990).
[4] J. Riess, Physica B **190,** 366 (1993) and references quoted therein.
[5] U. Klass, W. Dietsche, K. von Klitzing, and K. Ploog, Z. Phys. B **82,** 351 (1991); Surf. Sci. **263,** 97 (1992); U. Klass, Thermographie des Quanten-Hall-Effekts, Thesis, Eberhard-Karls-Universität Tübingen, Max-Planck-Institut für Festkörperforschung, Stuttgart 1992.
[6] A. Boisen, P. Boggild, A. Kristensen, and P. E. Lindelof, Phys. Rev. B **50,** 1957 (1994); A. A. Allerman, W. Xu, N. Hauser, and C. Jagadish, J. Appl. Phys. **77,** 2052 (1995).
[7] G. Hein, P. Schneider, L. Schweitzer, F. J. Ahlers, L. Bliek, H. Nickel, R. Lösch, and W. Schlapp, Surf. Sci. **263,** 293 (1992).
[8] M. E. Cage, G. Marullo-Reedtz, D. U. Yu, and C. T. van Degrift, Semicond. Sci. Technol. **5,** 351 (1990).
[9] F. J. Ahlers, G. Hein, H. Scherer, L. Bliek, H. Nickel, R. Lösch, and W. Schlapp, Semicond. Sci. Technol. **8,** 2062 (1993).
[10] G. Bella, L. Cordiali, G. Marullo-Reedtz, D. Allasia, G. Rinaudo, M. Truccato, and C. Villavecchia, Phys. Rev. B **50,** 7608 (1994).
[11] S. Komyiama, T. Takamasu, S. Hiyamizu, and S. Sasa, Solid State Commun. **54,** 479 (1985).
[12] J. Riess, Physica B **204,** 124 (1995).
[13] J. Riess and P. Magyar, Physica B **182,** 149 (1992).
[14] A. Messiah, Quantum Mechanics, North Holland, Amsterdam, (John Wiley & Sons, Inc., New York 1966), Vol. II, Chapt. XVII.
[15] J. von Neumann and E. Wigner, Phys. Z. **30,** 467 (1929).
[16] J. Riess, Z. Phys. B **77,** 69 (1989); D. Bicout, P.-A. Hervieux, and J. Riess, Phys. Rev. B **45,** 9577 (1992) and references quoted therein.
[17] J. Peinke, W. Clauss, R. P. Huebener, A. Kittel, J. Parisi, U. Rau, and R. Richter, in "Spontaneous Formation of Space-Time Structures and Critically", T. Riste and D. Sherrington (eds.), 145 (1991), Kluwer Academic Publishers, Netherlands.